

Laser and Ultrasound Activated Photolon Nanocomposite in Tumor-Bearing Mice: New Cancer Fighting Drug-Technique

Samir Ali Abd El-karem¹, Gihan Hosny Abd Elsamie², Ghufraan Abbas Isewid³

¹Lecturer of Applied Medical Chemistry, Medical Research Institute, Alexandria University, Egypt.

²Professor of Public Health & Occupational Medicine, Institute of Graduate Studies and Research Alexandria University, Egypt.

³B.Sc. of Medicine & Veterinary Surgery, College of Veterinary Medicine, University of AL-Qadisiyah, Iraq. Samir_ali852006@yahoo.com

***Corresponding Author:** Dr. Samir Ali Abd El-Kaream, M.Sc., Ph.D., Lecturer, Department of Applied Medical Chemistry, Medical Research Institute, Alexandria University-Egypt.

Abstract

This study was directed at study the effectiveness of cancer targeted therapy using the activated photolon nanocomposite (Nano-PhLon). Study was applied on male Swiss albino mice, implanted with Ehrlich tumor (EAC) divided into six groups. Two energy sources were used; laser and Ultrasound. Results showed that Nano-PhLon is a potential sensitizer for photodynamic or sonodynamic treatment of tumor. Nano-PhLon plays an important role in tumor growth inhibition and cell death induction. Activated Nano-PhLon with both infrared laser and ultrasound has a potential antitumor effect. The results indicated that (FA-NGO-PhLon) could be used as a unique nanocomposite for cancer targeted therapy SPDT.

Keywords: *implanted tumor; Nano-photolon; sonodynamic therapy; photodynamic therapy.*

INTRODUCTION

Cancer is one of the greatest challenges to researcher of our time. The objectives are to improve not only the therapeutic outcome, in advanced and metastatic cancer patients, but also treatment methods, which often have significant unfavorable effects [1, 2]. Currently, the main therapeutic approaches used to treat cancer are surgery, chemotherapy, and radiotherapy, delivered separately or in various combinations. Surgery and radiotherapy are key players for treating primary non-metastatic solid tumors, but for patients with co-morbidities that are unfit for surgery, deep-seated tumors, especially those associated with major blood vessels, or brain tumors, combined chemotherapy approaches are common. In chemotherapy, pharmaceutical compounds that exert a cytotoxic effect disrupting mechanisms underpinning the rapid overgrowth of malignant cells are administered. Conventional chemotherapy is effective but also well-known for its severe side effects

owing to the partially non-selective uptake of the chemotherapeutics both into healthy and cancerous cells in tissues and organs. Radiation therapy is a basic and beneficial treatment in treating about half of all cancer cases. This method depends on the deposition of energy in the tumor cells, usually by radiation either gamma rays or photons, or beams of active radiation, which are sufficient to damage cancer cells or blood vessels and thus stimulate tumor death or famine with nutrients. However, such as chemotherapy, photon irradiation therapy is undetermined, where a large dose can be transferred to normal tissue along the path of the photons, in front and back of the tumor [3, 4].

In recent years, there has been increasing interest in using of photodynamic therapy [PDT] to treat different types of cancers, either on its own or in combination with other anticancer treatment methods. PDT involve the administration of a photosensitizing (PS) drug and subsequently illuminating the target area with light

Laser and Ultrasound Activated Photolon Nanocomposite in Tumor-Bearing Mice: New Cancer Fighting Drug-Technique

corresponding to the absorbance wavelength of the PS, triggering a series of biological effects [5-8].

Sonodynamic therapy [SDT] has been raised as a promising noninvasive approach derived from PDT. The low penetration depth of light, PDT is not effective for the treatment of deep tumors. A great advantage of SDT on a PDT is that it can penetrate soft tissue up to tens of centimeters therefore; SDT overcomes the limitation of PDT [9-12].

Sono-photodynamic therapy [SPDT] is a new therapeutic method that utilizes a safe agent with sono and photo sensitive properties. PDT and SDT have been applied for years as separate processes for the treatment of cancer with variable results. PDT alone is used for more superficial tumor; but when combined with SDT, it has been shown to be efficient for deep-seated as well as metastatic tumors [13].

The aim of this work was to study the effectiveness of nano-photolon in activated cancer-targeted therapy. To achieve our goal the following was done:

Synthesis of nanographene oxide (NGO), conjugation of folic acid with nanographene oxide (FA-NGO) and photosensitizer photolon loading on FA-NGO (FA-GO-PhLon) according to modified Hummer's method [14], In the present work photolon was used as sonophotosensitizer; chemically active by absorption of light and/or ultrasound. photolon was purchased from Molbase Chemicals Co. India. The sonophotosensitizer obtained as powder stored in dark bottle at -20°C temperature and with Purity: 99.9% by HPLC analysis. PhLon was dissolved in a sterilized phosphate buffer saline solution with PH = 7.4 and mixed with FA-NGO (0.5 mg/mL) at room temperature for 24 h. The loading efficiency of PhLon was approved using UV absorbance at 663 nm. FA-NGO-PhLon administered to tumor-bearing mice intraperitoneally (IP) injection for 15 days 18-20 hours before exposure to either photo and/or sonodynamic treatment modality.

Experimental Design and Tumor Implantation

study was conducted on One hundred and thirty male Swiss albino mice. Ehrlich ascites carcinoma tumor cells, 2×10^6 human female mammary cells in origin, diluted approximately ten times in 0.9 % saline were inoculated subcutaneously on the left abdominal region of mice purchased from national cancer

institute, cairo university. The animals were housed in plastic cages and were kept under natural light with diet and water at available. When tumors reach to 10 mm in diameter on day 10 after implantation, the treatment study was started. Use of experimental animals in the study protocol was carried out in accordance with the ethical guidelines of the medical research institute, alexandria university (Guiding Principles for Biomedical Research Involving Animals, 2011). Mice were grouped into the following:

Group I: (30 mice); a) 10 mice: Control without tumor, **b) 10 mice:** Tumor bearing mice without treatment, **c) 10 mice:** Tumor bearing mice treated with (FA-NGO- PhLon) only.

Group II: (20 mice, laser irradiated group); a) 10 mice: were exposed to Infra-Red Laser, 4000Hz, for 3 minutes, **b) 10 mice:** were exposed to Infra-Red Laser, 7000Hz, for 3 minutes.

Group III: (20 mice, ultrasound group); a) 10 mice: were exposed to pulsed ultrasound for 3 minutes, **b) 10 mice:** were exposed to continuous ultrasound for 3 minutes.

Group IV: (20 mice, (FA-NGO-PhLon), laser group); Tumor bearing mice of this group were injected (IP) with (FA-NGO- PhLon), then the tumor sites were irradiated to laser light at same conditions of group II.

Group V: (20 mice, (FA-NGO- PhLon), ultrasound group); Tumor bearing mice of this group were injected (IP) with (FA-NGO- PhLon), then were divided into 2 sub-groups. The tumor sites were irradiated to ultrasound at same conditions of group III.

Group VI: (20 mice, combined treatment groups); a) 10 mice: were irradiated to laser light for 3 minutes, followed by ultrasound for 3 minutes, **b) 10 mice:** Injected (IP) with (FA-NGO-PhLon), then tumor sites were irradiated to laser light (7000 Hz) for 3 min, followed by pulsed ultrasound for 3 minutes.

Laser/Ultrasound Exposure

For laser and/or ultrasound exposure, the mice were anesthetized with diethyl ether. The hair over the tumors was shaved off. The mice were fixed on a board with the tumor upwards. The probe was placed nearly on the tumor, which was irradiated with laser and/or ultrasound for 3 minutes at the different conditions as mentioned before. After PDT, SDT and SPDT, animals

Laser and Ultrasound Activated Photolon Nanocomposite in Tumor-Bearing Mice: New Cancer Fighting Drug-Technique

were maintained in the dark to avoid skin irritation. Exposure of mice tumor to the laser beam was carried out using an Infrared diode laser, model LAS 50- Hi-Tech fysiomed, Germany operated at a wavelength of 904 nm and a peak power of 50 W at a frequency up to 7000 Hz. Exposure of mice tumor to the continuous and pulsed ultrasound was carried out using an ultrasonic therapy instrument (Model CSI Shanghai, No. 822 Factory. China). This instrument uses electronic tube to generate an electric oscillation with frequency 0.8 MHz and power output which converted to ultrasonic mechanical energy by means of ultrasonic transducer (calcium zirconate -titanate). The mechanical ultrasonic energy has a beam power density which can be adjusted from 0.5 to 3W/cm². This instrument operates at both continuous wave mode with output power from 0.5 - 3W/cm² adjustable in 11 steps and pulsed mode (pulse frequency 1000 Hz, duty ratio 1/3 and average power density from 0.15-1 W/cm²).

For evaluation of the treatment effects to all studied groups the following investigations were done:

Tumor Growth / Inhibition Assay

During treatment session, tumor growth was examined regularly every day. Length and width of tumors were measured with a slide caliper and tumor volume (in mm³) was calculated by the use of the following equation. $TV (mm^3) = 22/7 \times 4/3 \times (\text{length}/2) \times (\text{width}/2)^2$

Two weeks after the treatment, the mice were sacrificed and the tumors were dissected out, weighed (in grams). The tumor volume growth ratio and tumor mass inhibition ratio were calculated as follows. $TMIR=1 - (\text{average tumor weight of treated group} / \text{average tumor weight of control group}) \times 100$

Biochemical Examination

Blood sample (2.5 ml of venous blood) was withdrawn from all mice group. This blood samples were allowed to clot thoroughly for 20 minutes then centrifuged at 3000xg for 20 minutes for separating serum for biochemical examinations. All biochemical analysis was done on Indiko Plus Auto-analyzer.

Oxidative Stress and Antioxidant Profile

Lipid peroxidation (MDA) assay kit (BioVision Catalog # K739-100), total antioxidant capacity (TAC) assay

kit (BioVision Catalog #K274-100), glutathione reductase (GR) activity assay kit (BioVision Catalog #K761-100), glutathione-s-transferase (GST) activity assay kit (BioVision Catalog #K263-100), superoxide dismutase (SOD) activity assay kit (BioVision Catalog #K335-100), Catalase (CAT) activity assay kit (BioVision Catalog #K773-100), were used according to the manufacturer's instructions.

Kidney and Liver Biomarkers

Urea (Sigma Catalog # MAK179), creatinine (Sigma Catalog# MAK080), Alanine Transaminase (ALT) Activity Assay Kit (Sigma Catalog# MAK052), Aspartate Aminotransferase (AST) Activity Assay Kit (Sigma Catalog #MAK055) and ©-Glutamyltransferase (GGT) Activity Assay Kit (Sigma Catalog #MAK089), were used according to the manufacturer's instructions.

Molecular Detection of Survivin mRNA Gene Expression in Excised Tumor via RT-PCR

RNA was extracted from the Erich tumor of mice using QIAamp RNA tissue kit, was purchased from QIAGEN, USA according to the manufacturer's instructions. Preparation of Full-Length First strand cDNA from RNA template using RevertAid™ First cDNA Strand Synthesis Kit. Reverse transcription reaction was carried out in a 20 µl reaction mixture by using Revert Aid™ First cDNA Strand Synthesis Kit # K1621, #1622, was purchased from MBI Fermentas, Lithuania according to manufacturer's instruction. For amplification; to each PCR tube the following were added 5 µl (0.25 µg) Template *survivin* - cDNA, 10 µl Taq™ Green PCR Master Mix (2X) {dNTPs [0.4 mM of each dATP, dCTP, dGTP, dTTP], 0.05u/µl Taq DNA polymerase and reaction buffer} # k1081, was purchased from MBI Fermentas, Lithuania, 1.5 µl *survivin* forward primer: 5-TGAGCTTCTGCATTGGGAG-3', 1.5 µl *survivin* reverse primers: 5-CCCGCCAGCATCATAGCTTA-3' and deionized-RNase free water to final volume 20 µl. The reaction mixtures were gently vortexed, briefly centrifuged to collection all drops to the bottom of the tubes, then were placed in the thermal cycler (Little Genius, Bioer Co), The PCR mixture was subjected to 35 amplification cycles. PCR thermal profile was as follow: pre-denaturation (94°C, 2min), followed by 35 cycles of denaturation (94°C, 1min), annealing

Laser and Ultrasound Activated Photolon Nanocomposite in Tumor-Bearing Mice: New Cancer Fighting Drug-Technique

(52°C, 1min), and extension (72°C, 1min), with a final extension (72°C, 7min). To verify the successful preparation of mRNA and as positive controls, samples were detected for the presence of glyceraldehyde-3-phosphate dehydrogenase (*GAPDH*) mRNA. Forward primer: 5-AGGCCGGTGCTGAGTATGTC-3; reverse primers: 5-TGCCTGCTTCACCACCTTCT-3. Reaction tubes containing no cDNA control template and without cDNA sample addition were included as negative controls for each PCR reaction. For detection; Amplicons were analyzed with 2% (wt/vol) ethidium bromide stained agarose gel. The bands were visualized on a 302 nm UV transilluminator (BIO-RAD, USA). The gel was examined for bands of 254bp and 530bp as determined by the molecular weight marker (Gene Ruler™ 100bp DNA marker #SM0323, was purchased from Fermentas, Lithuania) runs at the same time and then photographed using a digital camera.

Histopathological Examination

Small pieces of Ehrlich tumor tissue of the experimental groups were processed and examined by haematoxylin and eosin (H&E) method as follows; small pieces of Ehrlich Tumor tissues were fixed at 10% formaldehyde, dehydrated in ascending grades using alcohol, embedded in paraffin to produce paraffin block, the blocks were cut into 3-4 µm thick sections and floated in water bath, cleaned with xylene, rehydrated in descending grades of alcohol, stained with haematoxylin and eosin stain, cleaned again ethylene and covered by covering slides, thus the slides were prepared to be examined by light microscopy.

Statistical Analysis of Data

The findings were presented using one-way variance analysis (ANOVA). Results were expressed as mean ± standard deviation (SD) and values of $P > 0.05$ were considered non-significantly different, while values of $P < 0.05$ were assumed significant. F probability expresses the general effect between groups.

RESULTS

Treatment with NPhLon without activation has little or no effect on tumor volume and tumor weight. Up to one week, all treatment modulates have little effect on the tumor volume and tumor weight. After one

week, treatment with IRL and ultrasound (pulsed or continuous wave) in the presence or absence of NPhLon, become more effective. The presence of NPhLon increases the effect of both IRL and ultrasound. Results obtained indicated that pulsed ultrasonic wave is more effective than continuous ultrasonic wave in the presences of NPhLon. Pulsed wave ultrasound at 3W/cm² was selected to combine with IRL at 7000 Hz. This combined treatment modality is more effective on tumor cells than using of infrared laser (IRL) or ultrasound alone. Figure (1-3)

Oxidative Stress and Antioxidant Profile

In our study, the increase in lipid peroxidation was reported in controlled group which carried EAC. In all the irradiated groups and that irradiated and treated without NPhLon, a significant increase in the levels of MDA was observed. Animals in groups irradiated with IRL or U.S or both with NPhLon exhibited significantly low levels of MDA, as compared with the cancer control group or with treated mice without activation of NPhLon, Figure (4). The same table, the implanted mice with EAC showed decreased activities of antioxidants (SOD, CAT, GR, GST and TAC) in comparison with normal animals. On the other hand, there is a significant increase in the enzymatic and non-enzymatic antioxidant guard in the groups irradiated with IRL or US or both with NPhLon when compared with cancer control group or with treated mice without activation of NPhLon.

Kidney and Liver Biomarkers

The renal function tests, namely; creatinine and urea, were estimated. The EAC caused a significant increase in the serum urea and creatinine levels in the studied groups. On the other hand the NPhLon caused decrease in the levels of serum creatinine and urea which is probably an indication of renal protection, Figure (5). This also confirms the protective role of NPhLon against renal toxicity. Also the hepatic function tests, ALT, AST and GGT, were estimated. The EAC caused a significant increase in the serum activities of ALT, AST and GGT of the tumor treated groups. However, in the EAC treated groups with NPhLon a decrease in serum levels of ALT, AST, and GGT, were observed which is an indication of the hepatoprotection by NPhLon, i.e., this confirms the protective role of NPhLon against hepatotoxicity.

Laser and Ultrasound Activated Photolon Nanocomposite in Tumor-Bearing Mice: New Cancer Fighting Drug-Technique

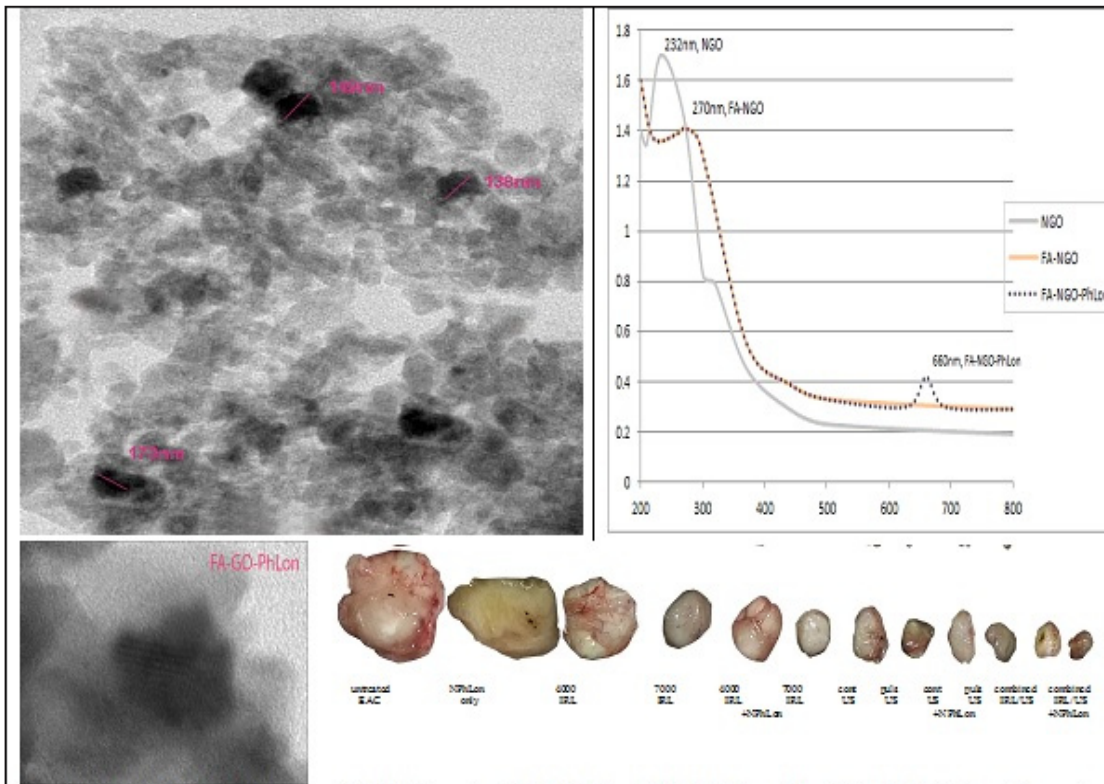


Figure (1): TEM of FA-GO-PhLon nanoparticle, UV-vis spectra of GO, FA-GO and FA-GO-PhLon and the effect of IRL at different frequencies, US continuous / pulsed and Combined modalities on the tumor volume (mm³), of untreated and NPhLon treated groups.

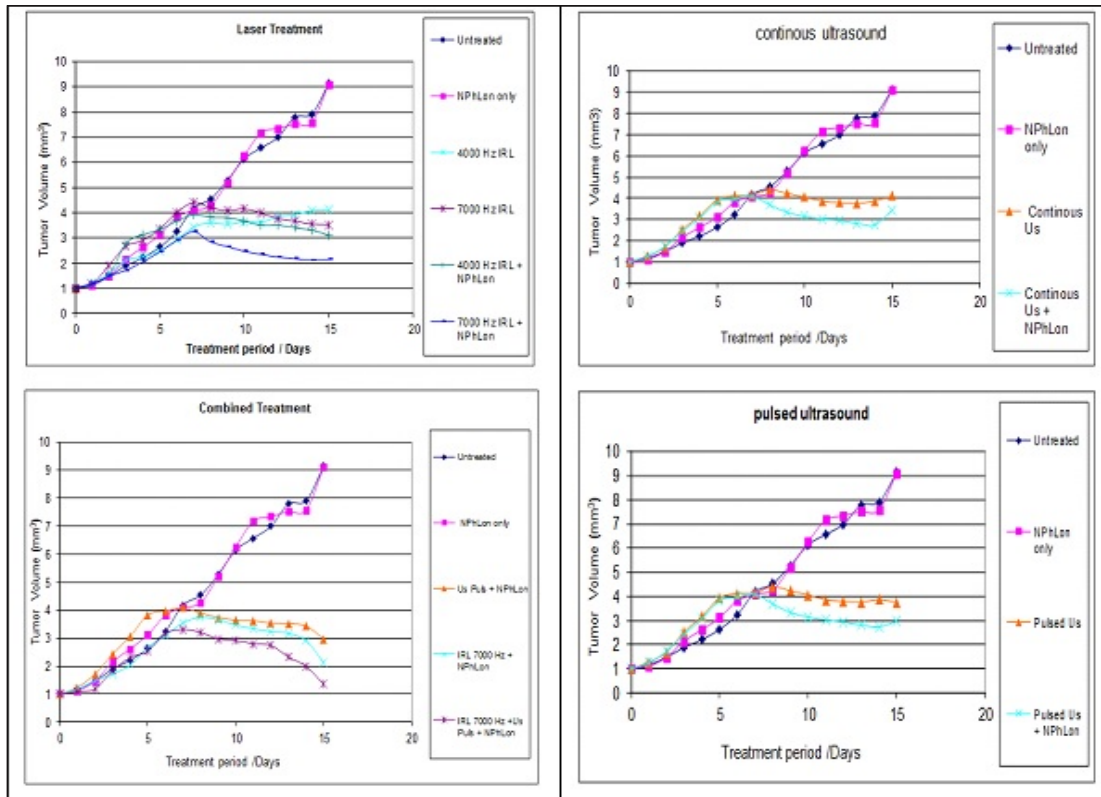


Figure (2): The effect of IRL at different frequencies, US continuous / pulsed and Combined modalities on the tumor volume (mm³), of untreated and NPhLon treated groups during treatment period.

Laser and Ultrasound Activated Photolon Nanocomposite in Tumor-Bearing Mice: New Cancer Fighting Drug-Technique

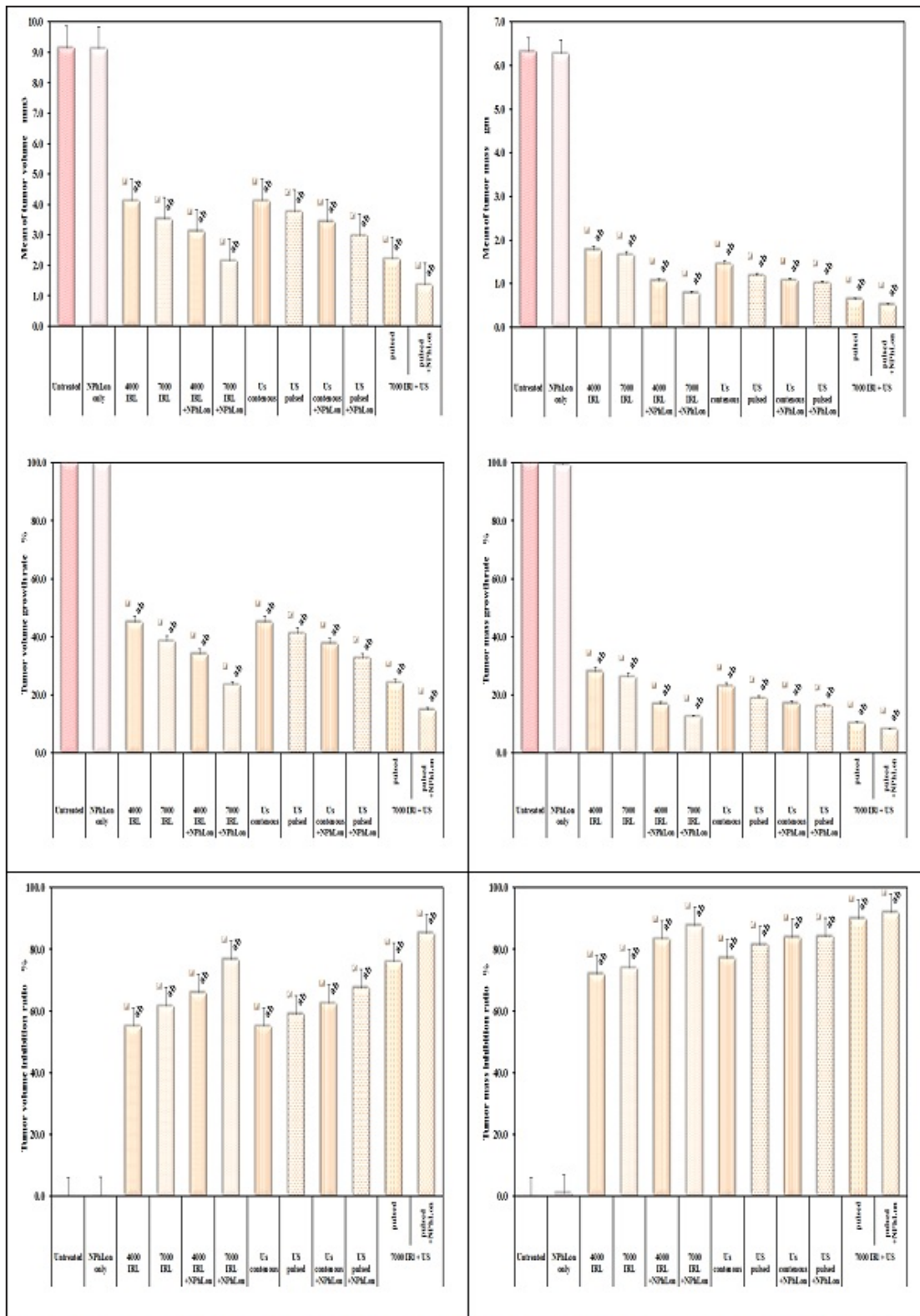
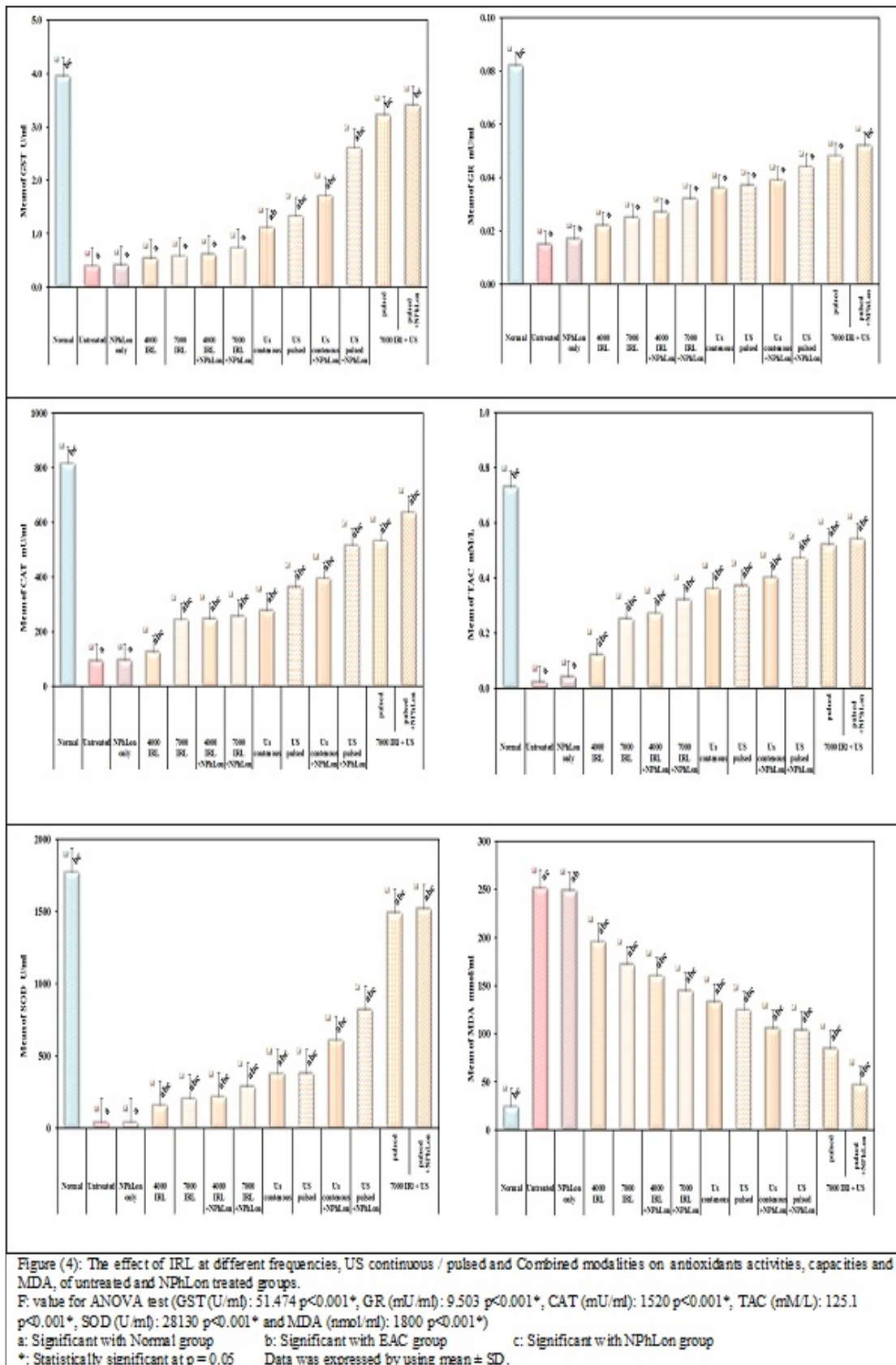


Figure (3): The effect of IRL at different frequencies, US continuous / pulsed and Combined modalities on the tumor volume (mm³), tumor volume growth rate (%), tumor volume inhibition ratio (%), tumor mass (gm), tumor mass growth rate (%), tumor mass inhibition ratio (%), of untreated and NPhLon treated groups.

F: F value for ANOVA test TV (mm³): 50.258 p<0.001*, TM (gm): 29.179 p<0.001*

a: Significant with EAC group b: Significant with NPhLon only group * : Statistically significant at p = 0.05

Laser and Ultrasound Activated Photolon Nanocomposite in Tumor-Bearing Mice: New Cancer Fighting Drug-Technique



Laser and Ultrasound Activated Photolon Nanocomposite in Tumor-Bearing Mice: New Cancer Fighting Drug-Technique

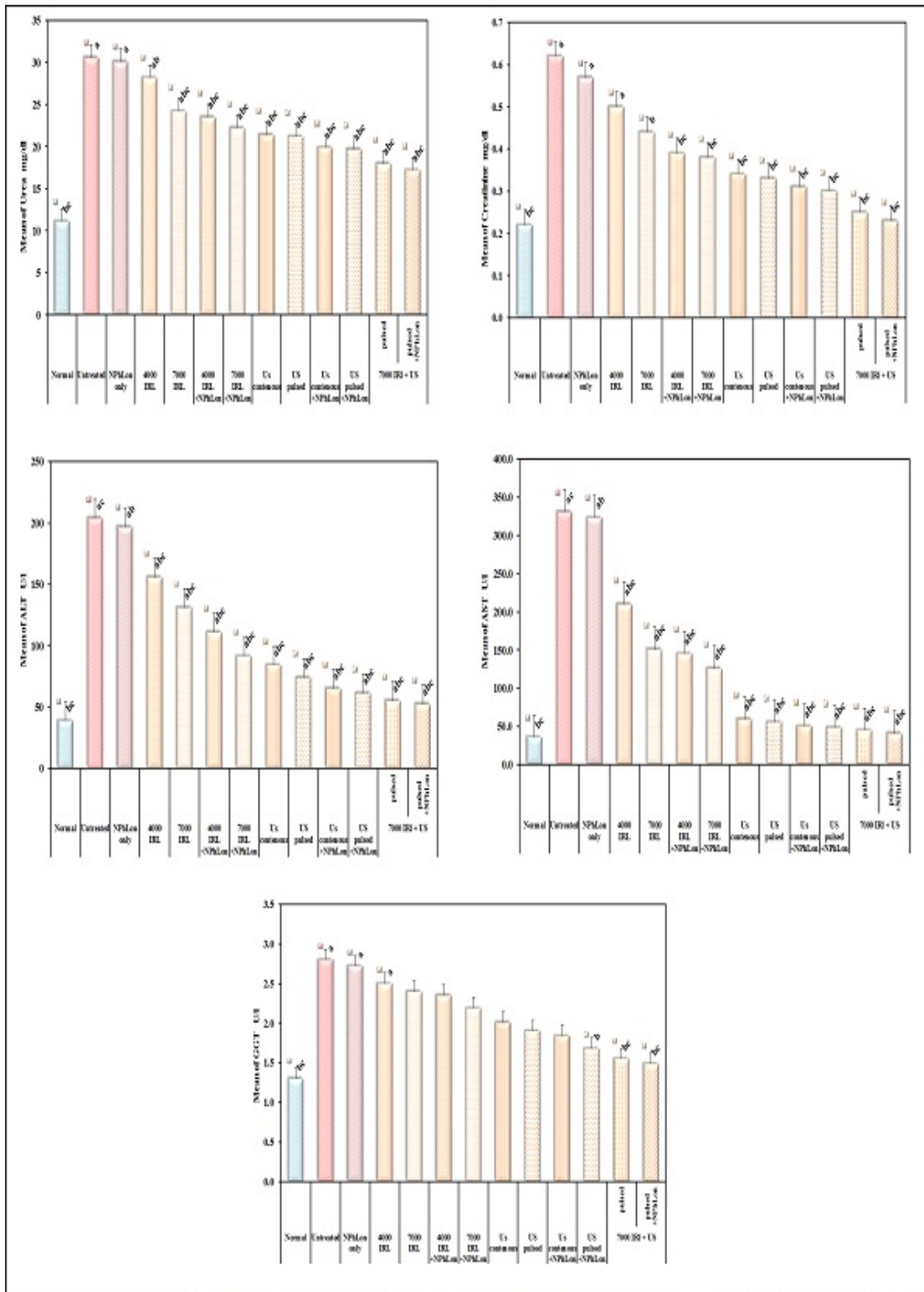


Figure (5): The effect of IRL at different frequencies, US continuous / pulsed and Combined modalities on renal and hepatic biomarkers, of untreated and NPhLon treated groups.

F. value for ANOVA test (Urea (mg/dl): 225.476 $p < 0.001$ *, Creatinine (mg/dl): 6.213 $p < 0.001$ *, ALT (U/l): 421.4 $p < 0.001$ *, AST (U/l): 8071 $p < 0.001$ * and GGT (U/l): 4.478 $p < 0.001$ *)

a: Significant with Normal group

b: Significant with EAC group

c: Significant with NPhLon group

*: Statistically significant at $p = 0.05$

Data was expressed by using mean \pm SD.

Histological Evaluation

The histological evaluation revealed that all tumors from the group of mice bearing tumor without treatment working as a control group were highly malignant cells and the tumors showed 5-10 % necrosis. Group of mice bearing tumor treated with (NPhLon) only the similar percentage as only EAC group due to NPhLon inactivation, Group of mice bearing tumor treated with 4000Hz, 7000Hz IRL only, showed significant areas of necrosis (40- 55% respectively). In the group of mice injected IP with (NPhLon) then the tumor site were irradiated to 4000Hz, 7000Hz showed significant areas of necrosis (56-67% respectively).

Group of mice bearing tumor treated with continuous and pulsed ultrasound showed significant areas of necrosis (55- 60% respectively).The group of mice injected IP with (NPhLon), then the tumor site was irradiated to continuous and pulsed ultrasound the areas of necrosis (65- 75% respectively), when compared with EAC untreated group. In case of two combination groups, mice bearing tumor treated 7000Hz followed by pulsed ultrasound only, and mice bearing tumor injected IP with (NPhLon) then tumor site was irradiated to 7000Hz, followed by pulsed ultrasound, large foci of necrosis areas (80- 82% respectively) were present which were distinctly appeared. Figure (6)

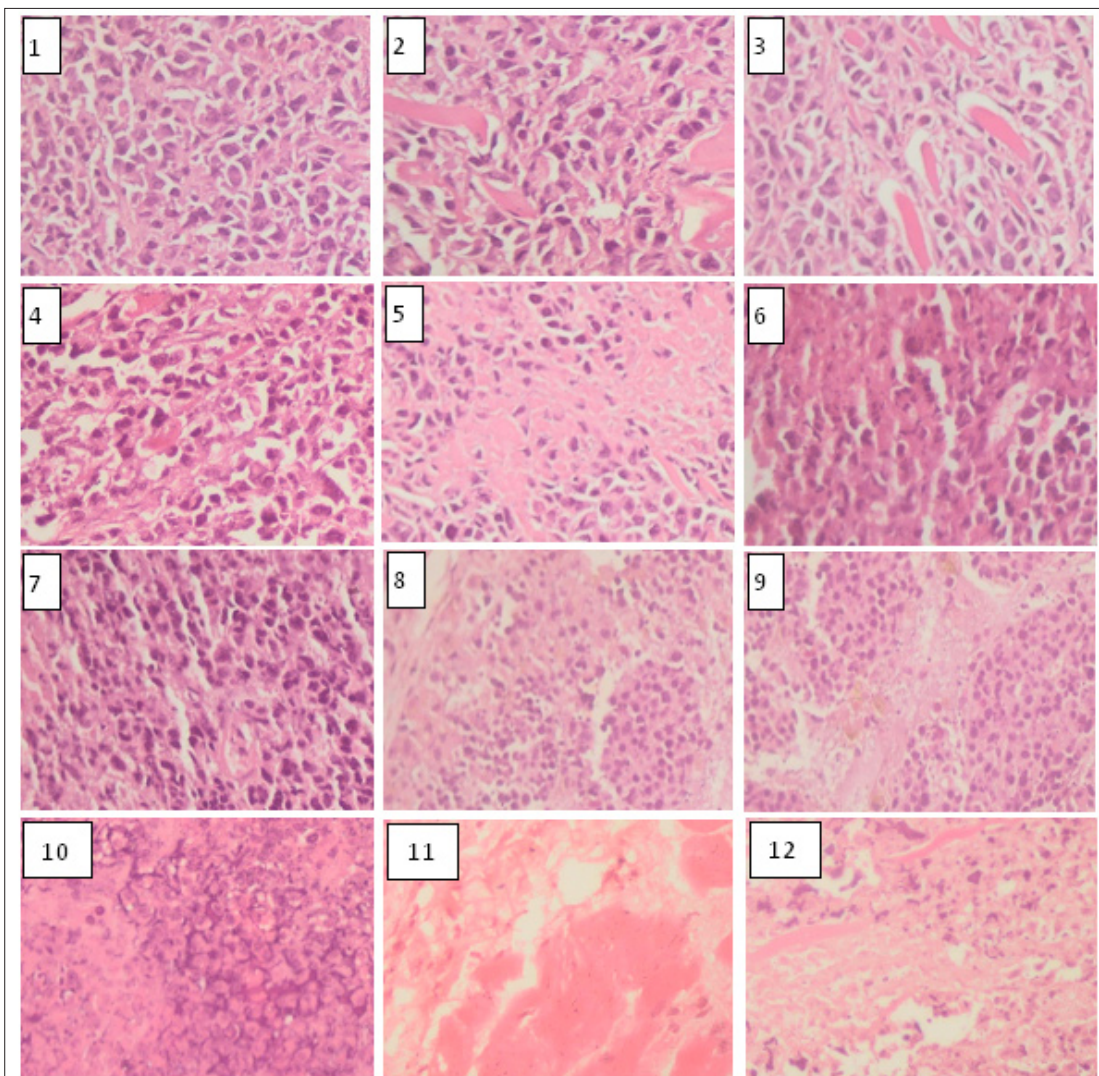


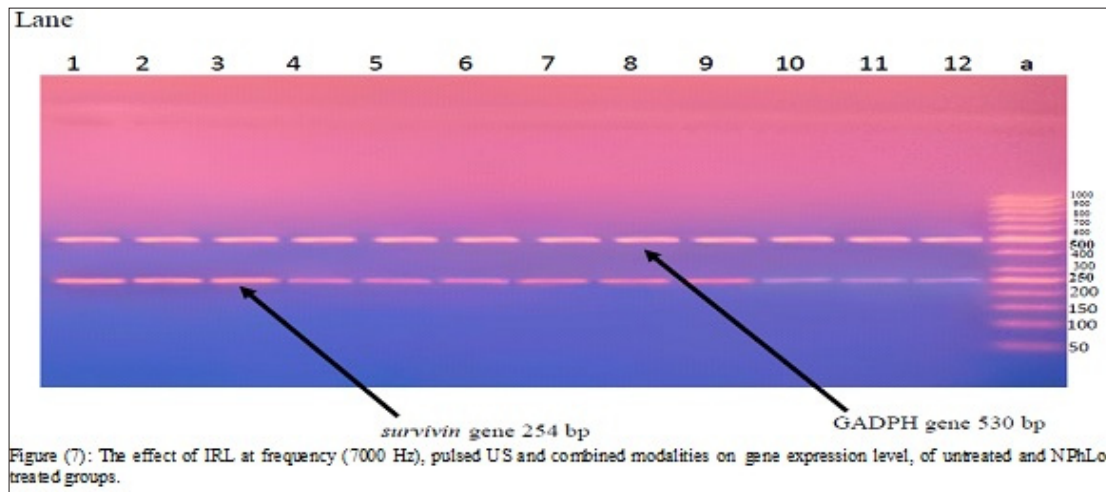
Figure (6): The histopathological evaluation of 1; untreated EAC implanted group without any treatment, 2; NPhLon treated group without activation, 3;4000 Hz IRL in absence of NPhLon, 4;7000 Hz IRL in absence of NPhLon, 5;4000 Hz IRL in presence of NPhLon, 6;7000 Hz IRL in presence of NPhLon, 7;continuous US in absence of NPhLon, 8;pulsed US in absence of NPhLon, 9;continuous US in presence of NPhLon, 10;pulsed US in presence of NPhLon, 11;Combined modalities IRL/US in absence of NPhLon and 12;Combined modalities IRL/US in presence of NPhLon on cellular level.

Laser and Ultrasound Activated Photolon Nanocomposite in Tumor-Bearing Mice: New Cancer Fighting Drug-Technique

Survivin Gene Expression

Amplification of *survivin* gene expression in breast tissues of all studied groups using RT-PCR is shown in Figure (7). PCR products were separated by 2% agarose gel electrophoresis. Products for *survivin* and *GADPH* gene expression were at 254 and 530 bp, respectively. Lane (a) is the molecular weight marker (50 bp DNA ladder). All samples were positive to

GADPH gene expression, while lanes (1-3), lanes (4-6), lanes (7-9), and lanes (10-12) with different intensity; showed positive bands of *survivin* gene expression, EAC cancerous untreated group, EAC cancerous group treated with laser, EAC cancerous group treated with ultrasound, EAC cancerous group treated with combined laser and ultrasound, respectively in presence of nano-PhLon.



DISCUSSION

In the present work, nano-PhLon as sono-photosensitizer, IR laser photodynamic therapy and sonodynamic therapy were employed to investigate whether alone or combined together, could be safely administered, provide an increased local tumor cytotoxic response and represents a promising approach in cancer therapy.

The MDA level is used as an indicator of oxidative stress, indicating an increasing interest in studying the role that lipid peroxidation played in the development of cancer. A low-molecular-weight aldehyde MDA is generated from free radical attack on polyunsaturated fatty acids [15, 16].

The probable cause of a high level of serum lipid peroxide in cancer may be due to a defective antioxidant system that leads to accumulation of lipid peroxides in the cancerous tissues followed by secretion in the bloodstream [17]. MDA is a product of high-toxic cytotoxic aldehydes of lipid peroxidation. It is said to inhibit protective enzymes. Thus, they can have both mutagenic and carcinogenic effects [18.]

In our study, the increase in lipid peroxidation was recorded during EAC which known with its carcinoge-

nicity. All groups injected with EAC, have a statistical significant elevation in the levels of MDA as compared to the control group animals. The inhibition of peroxidation by nano-PhLon is mainly attributed to the scavenging of the reactive free radicals involved in the peroxidation [19]. Animals in groups injected with nano-PhLon as a treatment showed significantly low levels of MDA, compared to animals not treated with nano-PhLon. This verifies the anti-lipid peroxidative role of nano-PhLon by its ability to scavenge free radical generation.

For the purpose of preventing cellular damage caused by ROS, there is a lot of anti-oxidant defense system. The antioxidant defense system may detect ROS, which plays an important role in the initiation of lipid peroxidation, thus playing a protective role in the development of cancer [20]. This defense system works through enzymatic (including SOD, GPx, GST and CAT) and non-enzymatic components (mainly GSH) [21, 22]. SOD is the basic step of the defense mechanism in an antioxidant system against oxidative stress, because it breaks down the superoxide anion (O_2^-) into O_2 and H_2O_2 . Gpx and catalase can delete

Laser and Ultrasound Activated Photolon Nanocomposite in Tumor-Bearing Mice: New Cancer Fighting Drug-Technique

H₂O₂ and convert it to harmless by-products, thereby providing protection against ROS [23.]

Also, GPX has a high strength in neutralizing reactivated free radicals in response to oxidative stress and detoxification of peroxides and hydroperoxides that lead to GSH oxidation [24]. Moreover, GST stimulates the coupling of functional groups of GSH atoms to electrophilic xenobiotics, leading to elimination or conversion of xenobiotic-GSH conjugate [25]. In such an interaction, GSH is oxidized into GSSG, which can be reduced to GSH by GR with NADPH consumption [26]. GSH is the most important non-enzymatic antioxidant in mammalian cells [27]. GSH is said to be involved in many cellular processes including detoxification of internal and external compounds and effectively protects cells against the harmful effects of oxidative stress by removing free radicals, removing H₂O₂, and suppressing lipid peroxidation [28].

In the present study, the EAC bearing mice showed decreased activities of antioxidants (SOD, CAT, GR, GST and TAC) in comparison with control animals. The present data are consistent with previous findings [29, 30]. Pradeep et al. (2007) [30] reported that such subsequent lower in the antioxidant defense is due to the low expression of these antioxidants during mammary gland damage. On the other hand, there is a significant increase in the enzymatic and non-enzymatic antioxidant guard in the animals which carried the EAC when treated with nano-PhLon, US and /or IRL when compared to the control group. This increase is due to the ability of nano-PhLon to prevent the formation of free radicals, enhance the endogenous antioxidant activity beyond its free radical scavenging property and the reduction of EAC lipoperoxide formation [31].

The increase in the activities of the antioxidant enzymes in the nano-PhLon treated mice compared to control group indicates its effect [32-41]. In this work, a statistically significant negative correlation between antioxidant activities and plasma mean levels of MDA was observed. The increased MDA level could be explained by defect in the antioxidant system with accumulation of lipid peroxides in the tumor as reported by Kumaraguruparan et al. (2002) [41] Furthermore, Sener et al. (2007) [42] found statistically significant decreased total antioxidant

capacity with significantly increased serum MDA levels in EAC group compared to control group.

Urea and creatinine are metabolic products that are cleaned of the blood circulation by the kidneys to prevent their accumulation. Increasing serum levels of these substances is an indication of kidney function loss [43, 44]. Data from this study suggest that mice groups implanted with EAC caused a loss of renal function compared with normal mice group and this is consistent with previous reports [45, 46]. The urea and creatinine, biomarkers of renal function, were assessed in this study. It was observed in the current study that nano-PhLon ameliorated the levels of serum urea and creatinine which is a marker of renal protection. This also indicates the protective role of nano-PhLon against mice groups implanted with EAC which induced renal dysfunction.

The liver is implicated in the biotransformation of drugs and toxicants. The serum level of bilirubin and activities of the ALT, AST, ALP, and GGT liver enzymes, are considered reliable indices of hepatotoxicity [47, 48]. Hepatocellular injury give rise to increase in serum ALT and AST [49]. Bilirubin is associated with liver, intestines, and spleen while ALP and GGT are associated with the cell membrane [50]. Serum bilirubin and activities of ALP and GGT increased in hepatobiliary injury [50]. The ALT, AST and GGT, biomarkers of hepatic function, were considered in this study. In this study, mice groups implanted with EAC caused increase in serum of ALT, AST and GGT activities. ALT and AST are present in the hepatocytes cytoplasm and mitochondria [51]. In this study, treatment with nano-PhLon protected against increase in serum of ALT, AST, and GGT levels, which is an indication of hepato-protection by nano-PhLon. This also confirms the protective role of nano-PhLon against hepato-dysfunction.

In the present work, study molecular study of *survivin* gene expression as a molecular diagnostic and prognostic markers for breast cancer revealed that there was a significantly negative correlation between modality of treatment and *survivin* gene expression in presence of nano-PhLon in treated groups while a positive correlation between *survivin* gene expression and cancer progression in untreated cancerous group. *Survivin* gene expression significantly lower in mice groups treated with

Laser and Ultrasound Activated Photolon Nanocomposite in Tumor-Bearing Mice: New Cancer Fighting Drug-Technique

sonophoto therapy (in presence of nano-PhLon) than those treated with photo- or sono-therapy only (in presence of nano-PhLon alone) followed by photo- or sono-therapy only (in absence of nano-PhLon alone) while the highest expression was among untreated cancerous group. The present results further support that molecular detection of *survivin* gene expression using RT-PCR could be used as a diagnostic and prognostic predictor of breast cancer and was in agreement with other studies done by other authors [52-61].

Finally, it can be concluded that the present study opened new trends for cancer treatment therapy that needs to be further verified. The study gave profound results involving the use of sono-photo-dynamic modality employing exposure to infra-red laser and ultrasound with (pulsed and continuous) in combination with nano-PhLon as a sono-photo sensitizer for treating Ehrlich tumor inoculated to mice as an experimental animals. The possible application of nano-carrier-sono-photo-dynamic therapy as *in vivo* anti-malignancy can open new line of research for modern cancer therapy that needs to be further investigated. Nanomaterial with their effective drug delivery great potential for can permit the feasibility of targeted therapy for disease treatment that needs further research for optimizing and maximizing benefits. Conjugated nanomaterial therapy can potentially provide a very valuable application for amplifying the benefits of photodynamic therapy. Response can be improved utilizing sonodynamic targeted therapy to treat deep or multiple lesions simultaneously. Further research is required to validate this novel therapy to prove feasibility and safety of application.

CONCLUSION

The present study gave profound results involving the use of sono-photo-dynamic modality employing exposure to infra-red laser and ultrasound with (pulsed and continuous) in combination with nano-PhLon as a sono-photo sensitizer for treating implanted Ehrlich tumor in mice as an experimental animals showing promising results for cancer treatment.

Recommendation

The present study opened new trends for cancer treatment therapy that needs to be further verified. It is

strictly recommended to conduct further experimental protocols aiming to safely apply this up-to-date modality on human and recording other biochemical and/or biophysical parameter's variations.

REFERENCES

- [1] Biemar, F., Foti, M., 2013. Global progress against cancer—challenges and opportunities. *Cancer Biol. Med.* 10,183–6.
- [2] Cagan, R., Meyer, P., 2017. Rethinking cancer: current challenges and opportunities in cancer research. *Dis. Model. Mech.* 10,349–52.
- [3] Schroeder, A., Heller, D.A., Winslow, M.M., Dahlman, J.E., Pratt, G.W., Langer, R., et al., 2012. Treating metastatic cancer with nanotechnology. *Nat. Rev. Cancer.* 12,39-50.
- [4] Ho, B.N., Pfeffer, C.M., Singh, A.T.K., 2017. Update on Nanotechnology-based Drug Delivery Systems in Cancer Treatment. *Anticancer. Res.* 37,5975-81.
- [5] Macdonald IJ, Dougherty TJ (2001) Basic principles of photodynamic therapy. *J Porphyrins Phthalocyanines* 5,105-29.
- [6] Castano AP, Demidova TN, Hamblin MR (2004) Mechanisms in photodynamic therapy: part one—photosensitizers, photochemistry and cellular localization. *Photodiagnosis Photodyn Ther* 1,279-93.
- [7] Mroz P, Yaroslavsky A, Kharkwal GB, Hamblin MR (2011) Cell death pathways in photodynamic therapy of cancer. *Cancers (Basel)* 3,2516-39.
- [8] Brodin NP, Guha C, Tomé WA (2015) Photodynamic therapy and its role in combined modality anticancer treatment. *Technol. Cancer Res Treat* 14,355-68.
- [9] Costley D, McEwan C, Fowley C, McHale AP, Atchison J, Nomikou N, et al (2015) Treating cancer with sonodynamic therapy: a review. *Int J Hyperthermia* 31, 107-17.
- [10] Su X, Wang P, Yang S, Zhang K, Liu Q, Wang X (2015) Sonodynamic therapy induces the interplay between apoptosis and autophagy in K562 cells through ROS. *Int J Biochem Cell Biol* 60, 82-92.
- [11] McEwan C, Owen J, Stride E, Fowley C, Nesbitt

- H, Cochrane D, et al (2015) Oxygen carrying microbubbles for enhanced sonodynamic therapy of hypoxic tumours. *J Control Release* 203,51-6.
- [12] Wan GY, Liu Y, Chen BW, Liu YY, Wang YS, Zhang N (2016) Recent advances of sonodynamic therapy in cancer treatment. *Cancer Biol Med* 13,325-38.
- [13] Miyoshi N, Kundu SK, Tuziuti T, Yasui K, Shimada I, Ito Y (2016) Combination of Sonodynamic and Photodynamic Therapy against Cancer Would Be Effective through Using a Regulated Size of Nanoparticles. *Nanosci Nanoeng* 4,1-11.
- [14] Paulchamy B, Arthi G, Lignesh BD (2015) A Simple Approach to Stepwise Synthesis of Graphene Oxide Nanomaterial. *J Nanomed Nanotechnol* 6:253.
- [15] Rao CSS, Kumari DS (2012). Changes in plasma lipid peroxidation and the antioxidant system in women with breast cancer. *Int J Basic Appl Sci* 1, 429-38.
- [16] Kumaraguruparan R, Subapriya R, Viswanathan P, Nagini S (2002) Tissue lipid peroxidation and antioxidant status in patients with adenocarcinoma of the breast. *Clin Chim Acta* 325, 165-70.
- [17] Ziech D, Franco R, Georgakilas AG, Georgakila S, Malamou-Mitsi V, Schoneveld O, et al (2010) The role of reactive oxygen species and oxidative stress in environmental carcinogenesis and biomarker development. *Chem Biol Interact* 188, 334-9.
- [18] Naser B, Bodinet C, Tegtmeier M, Lindequist U (2005) *Thuja occidentalis* (Arbor vitae): A Review of its Pharmaceutical, Pharmacological and Clinical Properties. *eCAM* 2,69-78.
- [19] López-Lázaro M (2008) Anticancer and carcinogenic properties of curcumin: Considerations for its clinical development as a cancer chemo preventive and chemotherapeutic agent. *Mol Nut Food Res* 52,103-27.
- [20] Zhang C, Zeng T, Zhao X, Yu L, Zhu Z, Xie K (2012) Protective effects of garlic oil on hepatocarcinoma induced by N-nitrosodiethylamine in rats. *Int J Biological Sci* 8, 363-74.
- [21] Chen B, Ning M, Yang G (2012) Effect of paeonol on antioxidant and immune regulatory activity in hepatocellular carcinoma rats. *Molecules* 17,4672-83.
- [22] Vásquez-Garzón V, Arellanes-Robledo J, García-Román R, Aparicio-Rautista DI, Villa-Treviño S (2009) Inhibition of reactive oxygen species and pre-neoplastic lesions by quercetin through an antioxidant defense mechanism. *Free Radic Res* 43, 128-37.
- [23] Usunomena U, Ademuyiwa A, Tinuade O, Uduenevwo F, Martin O, Okolie N (2012) N-nitrosodimethylamine (NDMA), liver function enzymes, renal function parameters and oxidative stress parameters: A Review. *Br J Pharmacol Toxicol* 3,165-76.
- [24] Rao G, Rao C, Pushpangadan P, Shirwaikar A (2006) Hepatoprotective effects of rubiadin, a major constituent of *Rubiocordifolia* Linn. *J Ethnopharmacol* 103,484-90.
- [25] Revathi R, Manju V (2013) The effects of Umbelliferone on lipid peroxidation and antioxidant status in diethylnitrosamine induced hepatocellular carcinoma. *J Acute Medicine* 3,73-82.
- [26] Wu G, Fang, YZ, Yang S, Lupton JR, Turner ND (2004) Glutathione metabolism and its implications for health. *J Nutr* 134,489-92.
- [27] Blair IA (2006) Endogenous glutathione adducts. *Curr Drug Metab* 7, 853-72.
- [28] Ghosh D, Choudhury ST, Ghosh S, Mandal AK, Sarkar S, Ghosh A, et al (2012) Nano capsulated curcumin: Oral chemopreventive formulation against diethylnitrosamine induced hepatocellular carcinoma in rat. *Chem Biol Interact* 195,206-14.
- [29] Rajeshkumar N, Kuttan R (2000) Inhibition of N-nitrosodiethylamine induced hepatocarcinogenesis by Picroliv. *J Exp Clin Cancer Res* 19, 459-65.
- [30] Pradeep K, Mohen, CV, Gobian K, Karthikeyan S (2007) Silymarin modulates the oxidant-antioxidant imbalance during diethylnitrosamine induced oxidative stress in rats. *Eur J Pharmacol* 560,110-16.
- [31] Ren W, Qiao Z, Wang H, Zhu L, Zhang L (2003)

- Flavonoids: promising anticancer agents. *Med Res Rev* 23,519-34.
- [32] Bemis D, Capodice J, Gorroochurn P, Katz A, Buttyananti R (2006) Anti-prostate cancer activity of a s-carboline alkaloid enriched extract from *Rauwolfia vomitoria*. *Int J Oncol* 29,1065-73.
- [33] Anne A, Grippo KC, Ben R, Bill J, Gurley C (2007) Analysis of flavonoid phytoestrogens in botanical and ephedra-containing dietary supplements. *Ann Pharmacother* 41,1375-82.
- [34] Jiang J, Hu C (2009) Evodiamine: a novel anti-cancer alkaloid from *Evodiarutaecarpa*. *Molecules* 14,1852-9.
- [35] Kabashima H, Miura N, Shimizu M, Shinoda W, Wang X, Wang Z, et al (2010) Preventive impact of alkaloids with anti-cancer effect extracted from natural herb and the derivatives. *Webmed Central* 1,1-19.
- [36] Thoppil R, Bishayee A (2011) Terpenoids as potential chemopreventive and therapeutic agents in liver cancer. *World J Hepatol* 3,228-49.
- [37] Kuno T, Tsukamoto T, Hara A, Tanaka T (2012) Cancer chemoprevention through the induction of apoptosis by natural compounds. *J Biophys Chem* 3,156-73.
- [38] Haghiac M, Walle T (2005) Quercetin induces necrosis and apoptosis in SCC-9 oral cancer cells. *Nutr Cancer* 53, 220-31.
- [39] Priyadarsini R, Murugan R, Maitreyi S, Ramalingam K, Karunagaran D, Nagini S (2010) The flavonoid quercetin induces cell cycle arrest and mitochondria-mediated apoptosis in human cervical cancer (HeLa) cells through p53 induction and NF- κ B inhibition. *Eur J Pharmacol* 649,84-91.
- [40] Bishayee K, Ghosh S, Mukherjee A, Sadhukhan R, Mondal JK, Bukhsh AR (2013) Quercetin induces cytochrome-c release and ROS accumulation to promote apoptosis and arrest the cell cycle in G2/M, in cervical carcinoma: signal cascade and drug-DNA interaction. *Cell Prolif* 46,153-63.
- [41] Kumaraguruparan R, Subapriya R, Kabalimoorthy J, Nagini S (2002) Antioxidant profile in the circulation of patients with fibroadenoma and adenocarcinoma of the breast. *Clin Biochem* 35, 275-9.
- [42] Sener D, Gönenç A, Akinci M, Torun M (2007) Lipid peroxidation and total antioxidant status in patients with breast cancer. *Cell Biochem Funct* 25,377-82.
- [43] Han W, Bonventre J (2004) Biologic markers for the early detection of acute kidney injury. *Curr Opin Crit Care* 10,476-82.
- [44] George G, Wakasi M, Egoro E (2014) Creatinine and urea levels as critical markers in end-stage renal failure. *Research and Review. J Med Heal Sci* 3,41-4.
- [45] Paliwal R, Sharma V, Pracheta, Sharma S, Yadav S, Sharma SH (2011) Antinephrotoxic effect of administration of *Moringaoleifera* Lam. in amelioration of DMBA-induced renal carcinogenesis in Swiss albino mice. *Biol Med* 3,27-35.
- [46] Sharma V, Paliwal R, Janmeda P, Sharma SH (2012) The reno-protective efficacy of *Moringaoleifera* pods on xenobiotic enzymes and antioxidant status against 7,12-dimethylbenz [a] anthracene exposed mice. *J Chin Integr Med* 10,1171-8
- [47] Boone L, Meyer D, Cusick P, Ennulat D, Bolliger AP, Everds N (2005) Selection and interpretation of clinical pathology indicators of hepatic injury in preclinical studies. *Vet Clin Pathol* 34,182-8.
- [48] Singh A, Bhat TK, Sharma OM (2011) Clinical biochemistry of hepatotoxicity. *J Clinic Toxicol* 4,1-19.
- [49] Ozer J, Ratner M, Shaw M, Bailey W, Schomaker S (2008) The current state of serumbiomarkers of hepatotoxicity. *Toxicology* 245,194-205.
- [50] Ramaiah S (2007) A toxicologist guide to the diagnostic interpretation of hepatic biochemical parameters. *Food Chem Toxicol* 45,1551-7.
- [51] Amacher D (2002) A toxicologist's guide to biomarkers of hepatic response. *Hum Exp Toxicol* 21: 253-62.
- [52] Ambrosini, G., Adida, C., Sirugo, G., Altieri, D.C., 1998. Induction of apoptosis and inhibition of cell proliferation by survivin gene targeting. *J. Biol. Chem.* 273,11177-82.

Laser and Ultrasound Activated Photolon Nanocomposite in Tumor-Bearing Mice: New Cancer Fighting Drug-Technique

- [53] Bao, R., Connolly, D.C., Murphy, M., Green, J., Weinstein, J.K., Pisarcik, D.A., et al., 2002. Activation of Cancer-Specific Gene Expression by the Survivin Promoter. *JNCI. J. Natl. Cancer Inst.* 94,522-8.
- [54] Kennedy, S.M., O'Driscoll, L., Purcell, R., Fitzsimons, N., McDermott, E.W., Hill, A.D., et al., 2003. Prognostic importance of survivin in breast cancer. *Br. J. Cancer.* 88,1077-83.
- [55] Ryan, B.M., Konecny, G.E., Kahlert, S., Wang, H.J., Untch, M., Meng, G., et al., 2006. Survivin expression in breast cancer predicts clinical outcome and is associated with HER2, VEGF, urokinase plasminogen activator and PAI-1. *Ann. Oncol.* 17,597-604.
- [56] Hinnis, A.R., Lockett, J.C., Walker, R.A., 2007. Survivin is an independent predictor of short-term survival in poor prognostic breast cancer patients. *Br. J. Cancer.* 96,639-45.
- [57] Guha, M., Altieri, D.C., 2008. Survivin as a global target of intrinsic tumor suppression networks. *Cell. Cycle.* 17,2708-10.
- [58] Mao, J.J., Palmer, C.S., Healy, K.E., Desai, K., Amsterdam, J., 2011. Complementary and alternative medicine use among cancer survivors: a population-based study. *J. Cancer. Surviv.* 5,8-17.
- [59] Jha, K., Kumar, M., Shukla, V.K., Pandey, M., 2012. Survivin Expression and Correlation with Clinicopathological Parameters in Breast Cancer. *World. J. Pathol.* 1,23-30.
- [60] Chi, Y., Wang, X., Yang, Y., Zhang, C., Ertl, H.C.J., Zhou, D., 2014. Survivin-targeting Artificial MicroRNAs Mediated by Adenovirus Suppress Tumor Activity in Cancer Cells and Xenograft Models. *Mol. Ther. Nuc. Acids.* 3,208.
- [61] Ma, W.H., Liu, Y.C., Xue, M.L., Zheng, Z., Ge, Y.L., 2016. Downregulation of survivin expression exerts antitumoral effects on mouse breast cancer cells in vitro and in vivo. *Oncol. Lett.* 11,159-67.

Citation: Samir Ali Abd El-karem, Gihan Hosny Abd Elsamie, Ghufan Abbas Isewid. *Laser and Ultrasound Activated Photolon Nanocomposite in Tumor-Bearing Mice: New Cancer Fighting Drug-Technique. Archives of Oncology and Cancer Therapy.* 2019; 2(1): 1-15.

Copyright: © 2019 Samir Ali Abd El-karem, Gihan Hosny Abd Elsamie, Ghufan Abbas Isewid. This is an open access article distributed under the Creative Commons Attribution License, which permits unrestricted use, distribution, and reproduction in any medium, provided the original work is properly cited.